2018 26th Mediterranean Conference on Control and Automation (MED)
Zadar, Croatia, June 19-22, 2018

Cooperative object transportation by two underwater vehicle-manipulator systems

Elisabetta Cataldi, Stefano Chiaverini, Gianluca Antonelli

Abstract— **Intervention Autonomous Underwater Vehicle, also denoted as interaction control of Underwater Vehicle-Manipulator Systems, is a topic receiving increasing attention in the last years due to the need to decrease costs and improve safety of underwater operations. From the control perspective the problem at hand is challenging due to the hostile environmental conditions. Cooperative control of underwater vehicle-manipulator systems is addressed in this paper. An architecture is proposed which takes into account most of the underwater constraints, namely, uncertainty in the model knowledge, low sensors' bandwidth, position-only arm control, geometric-only object pose estimation. Numerical simulations provide promising results on its possible real application.**

I. Introduction

Manipulation tasks —such, e.g., turning a valve, pushing a button, (un)plugging a connector, cleaning a surface or collecting a sample— involve interaction of an agent with the environment, that requires proper control of the force exchanged. In many cases the need arises of using more agents to execute a single task, leading to cooperative actions as shown in Figure 1. This occurs when, e.g., the object to be manipulated is heavy, long, thin or limp such that a single grasp would not suffice.

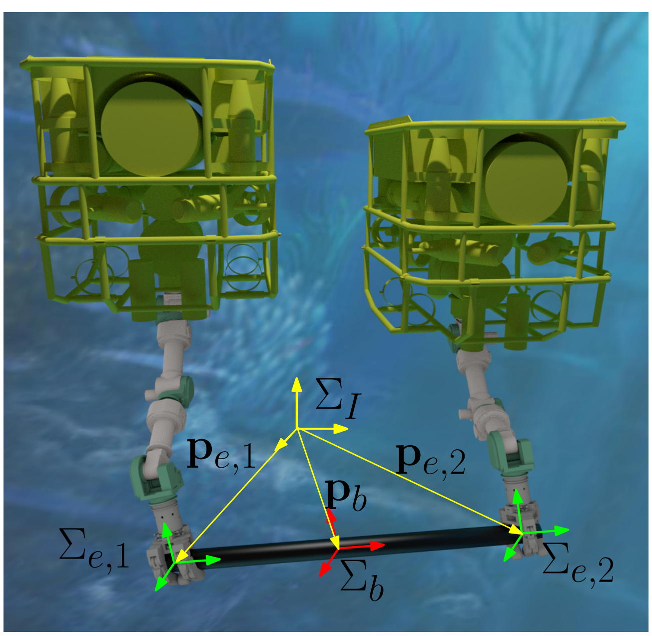

Fig. 1. Two UVMSs transporting a bar.

E. Cataldi, S. Chiaverini and G. Antonelli are with the DIEI—University of Cassino and Southern Lazio, via Di Biasio 43, 03043, Cassino, Italy {e.cataldi,chiaverini,antonelli}@unicas.it

In the latest years, there has been an increasing interest to underwater applications where the usual difficulty of controlling the motion of the manipulator and its interaction with the environment is increased by the need of using as agents floating robots under significant hydrodynamic effects.

Among different possible underwater vehicles, we will consider the class of Underwater Vehicle-Manipulator Systems (UVMSs). These are autonomous robotic systems undergoing several strong constraints that make challenging the control system's design, namely:

- Uncertainty in the model knowledge;
- Complexity of the mathematical model;
- Structural redundancy of the system;
- Difficulty to control the vehicle in hovering;
- Dynamic coupling between vehicle and manipulator;
- Low sensors' bandwidth.

Another issue to be taken into account in underwater intervention is the presence of redundant degrees of freedom, often present in such robotic systems. Among the first work handling both interaction and redundancy exploitation it is worth mentioning [14] which present a unified approach for motion and force control, extending the formulation to kinematically redundant manipulators. From the first proposed architectures, the control schemes have been further improved and experimentally tested, especially for industrial, ground manipulators. It is the case, e.g., of [16], [20]. It turns out, however, that most of the schemes requires knowledge of mathematical model together with the dynamic parameters in order to be properly implemented. In the underwater environment, mainly due to the presence of the hydrodynamic terms of added masses, damping and buoyancy, this assumption appears to be weak and basically unproven. As an additional issue, direct control of motor torques is needed while the off the shelf underwater arm are almost all hydraulic or position/velocity controlled at joints.

In [13] a very specific problem is approach, a floating vehicle, with a manipulator mounted on board, uses its thrusters and the resorting forces in order to apply the required force at the end effector, validation is achieved via numerical simulations. Another peculiar problem involving interaction is addressed in [25] in which fish-like robots are used to push a floating object toward a goal.

In [4] and [5] force control approaches have been proposed and numerically tested resorting to external and explicit control schemes, respectively.

The very first experiment run with two underwater arms, with fixed base, holding an object is given in [8], where

978-1-5386-7891-6/18/$31.00 ©2018 IEEE

the problem is decomposed in different layers of controllers. Reference [30] further extends this control problem and prove it with a numerical-only validation.

A test bench for laboratory reproduction of underwater interaction is proposed in [17].

In [24] the overall description of RAUVI, a Spanish research project, is given where an UVMS has the task to search and retrieve an object, a black-box in that case. Preliminary experiments in a pool with the grasp of the box are shown. Additional details of the design and software are in given in [11], [31] and, in the overall framework of the PANDORA European project, in [22]. In [23] an architecture for autonomous docking, then (un)plug and turn the valve by position-only control is proposed and validated by means of experiments in a pool. Experiments in an harbour at few meters depth have been achieved during the European project TRIDENT and a different arm and discussed in [29]. The approaches above do not implement yet an explicit force control scheme but interact with the environment by properly tuning position or velocity control. In fact, force sensors, when present, are not used to feedback the force signal.

In [21], a passivity-based model-free control scheme for a fully actuated UVMS in contact tasks is proposed. The main contribution is the design of a forcemotion control scheme to track desired pose, posture, and contact force trajectories with dexterity by a UVMS subject to an unknown dynamic model and known geometric constraints. Validation is achieved by means of numerical simulations.

Reference [12] presents a model-free control architecture aimed at force regulation of an UVMS in contact with a compliant environment validated by simulations.

The European project DexROV [10] is aimed at teleoperate an UVMS with the operator onshore and the explicit consideration of communication latency in the control loop. Teleoperation is also addressed in [15], with a torque-controlled arm and an impedance-based interaction loop. In the latter, the operator handles the UVMS by haptic feedback and wired connection.

Cooperation of two UVMS transporting an object is addressed, beyond the above mentioned [30], also in [18], [28], [27], [9] in which a unifying architecture for the control of both interaction control for a single UVMS and cooperation between two. Limited amount of communication exchange is taken into account. Validation is achieved by means of numerical simulations.

This paper addresses cooperative transportation of an object of known geometry but unknown mass by two UVMSs. The architecture is modular and complies with the severe constraints of the underwater environment as it will be detailed in Sect. III

II. Modeling

The notation used in this paper is shown in Table I.

Acronym	corresponding frame
$(\cdot)_I$	inertial
$(\cdot)_b$	bar
$(\cdot)_{v,i}$	i-th vehicle with $i=1,2$
$(\cdot)_{q,i}$	i-th manipulator with $i=1,2$
$(\cdot)_{e,i}$	i-th end-effector with $i=1,2$
$(\cdot)_{b,i}$	i-th bar ends with $i=1,2$
$(\cdot)_{x,int}$	$\boldsymbol{f},\boldsymbol{\mu}$ or $\boldsymbol{\tau}$ internal
x^{des}	desired of x

Symbol	corresponding variable
Σ_x	x frame
$\boldsymbol{p}_x$	x position $\in\mathbb{R}^3$ respect to the inertial frame
$\boldsymbol{R}_x$	rotational matrix respect to the inertial frame $\boldsymbol{R}_x^I\in\mathbb{R}^{3\times3}$
$\boldsymbol{\eta}_x$	x Euler angles $\in\mathbb{R}^3$ of $\boldsymbol{R}_x$
$\{\theta_x,\boldsymbol{r}_x\}$	x axis$\in\mathbb{R}^3$-angle$\in\mathbb{R}$ of $\boldsymbol{R}_x$
$\{\eta_x,\boldsymbol{\varepsilon}_x\}$	x quaternion of $\boldsymbol{R}_x$
$\boldsymbol{x}_x=\begin{bmatrix}\boldsymbol{p}_x^{\mathrm{T}} & \boldsymbol{\eta}_x^{\mathrm{T}}\end{bmatrix}^{\mathrm{T}}$	pose vector $\in\mathbb{R}^6$
$\boldsymbol{v}_x$	x linear velocity $\in\mathbb{R}^3$
$\boldsymbol{\omega}_x$	x angular velocity $\in\mathbb{R}^3$
$\boldsymbol{\nu}_x=\begin{bmatrix}\boldsymbol{v}_x^{\mathrm{T}} & \boldsymbol{\omega}_x^{\mathrm{T}}\end{bmatrix}^{\mathrm{T}}$	velocity vector $\in\mathbb{R}^6$
$\boldsymbol{f}_x$	x force $\in\mathbb{R}^3$
$\boldsymbol{\mu}_x$	x moment $\in\mathbb{R}^3$
$\boldsymbol{\tau}_x=\begin{bmatrix}\boldsymbol{f}_x^{\mathrm{T}} & \boldsymbol{\mu}_x^{\mathrm{T}}\end{bmatrix}^{\mathrm{T}}$	x wrench
$\boldsymbol{q}_i$	joint position vector $\in\mathbb{R}^n$, for an arm with n DoF
$\boldsymbol{\xi}_i=\begin{bmatrix}\boldsymbol{\nu}_{v,i}^{\mathrm{T}}\dot{\boldsymbol{q}}_i\end{bmatrix}^{\mathrm{T}}$	UVMS velocity vector $\mathbb{R}^{6+n}$
$\dot{x}$	x derivative

TABLE I

Acronyms and symbols used in this paper

A. Bar

The dynamic model of the bar can be modeled as a rigid body and written as form [26], [1]:

$$\boldsymbol{M}_b\dot{\boldsymbol{\nu}}_b+\boldsymbol{C}_b(\boldsymbol{\nu}_b)\boldsymbol{\nu}_b+\boldsymbol{D}_b(\boldsymbol{\nu}_b)\boldsymbol{\nu}_b+\boldsymbol{g}_b(\boldsymbol{R}_b)=\boldsymbol{\tau}_b, \quad (1)$$

where $\boldsymbol{M}_b\in\mathbb{R}^{6\times6}$ is the bar inertia matrix, $\boldsymbol{C}_b(\boldsymbol{\nu}_b)\boldsymbol{\nu}_b\in\mathbb{R}^6$ is the vector of Coriolis and centripetal terms including the added mass effects, $\boldsymbol{D}_b\boldsymbol{\nu}_b\in\mathbb{R}^6$ is the vector of friction and hydrodynamic damping terms, $\boldsymbol{g}_b(\boldsymbol{R}_b)\in\mathbb{R}^6$ is the vector of gravitational and buoyant wrench and $\boldsymbol{\tau}_b\in\mathbb{R}^6$ is the bar wrench.

B. Vehicle-manipulator

The UVMS is composed by a fully actuated vehicle and a n-DoF manipulator attached on the vehicle base. The UVMSs used are equal ($i=1,2$), then in the following the dynamic model of only one UVMS is reported:

$$\boldsymbol{M}_i(\boldsymbol{q}_i)\dot{\boldsymbol{\xi}}_i+\boldsymbol{C}_i(\boldsymbol{q}_i,\boldsymbol{\xi}_i)\boldsymbol{\xi}_i+\boldsymbol{D}_i(\boldsymbol{q}_i,\boldsymbol{\xi}_i)\boldsymbol{\xi}_i+\boldsymbol{g}_i(\boldsymbol{R}_i,\boldsymbol{q}_i)=\bar{\boldsymbol{\tau}}_i, \quad (2)$$

where $\boldsymbol{M}_i\in\mathbb{R}^{6+n\times6+n}$ is the system i inertia matrix, $\boldsymbol{C}_i(\boldsymbol{q}_i,\boldsymbol{\xi}_i)\boldsymbol{\xi}_i\in\mathbb{R}^{6+n}$ is the vector of Coriolis and centripetal terms including the added mass effects, $\boldsymbol{D}_i(\boldsymbol{q}_i,\boldsymbol{\xi}_i)\boldsymbol{\xi}_i\in\mathbb{R}^{6+n}$ is the vector of friction and hydrodynamic damping terms, $\boldsymbol{g}_b(\boldsymbol{R}_i,\boldsymbol{q}_i)\in\mathbb{R}^{6+n}$ is the vector of gravitational and buoyant wrench and $\bar{\boldsymbol{\tau}}_i=\begin{bmatrix}\boldsymbol{\tau}_{v,i}^{\mathrm{T}} & \bar{\boldsymbol{\tau}}_{q,i}^{\mathrm{T}}\end{bmatrix}^{\mathrm{T}}\in\mathbb{R}^{6+n}$ is the vector containing the vehicle applied wrench $\boldsymbol{\tau}_{v,i}\in\mathbb{R}^6$, and the manipulator's joint torque $\bar{\boldsymbol{\tau}}_{q,i}\in\mathbb{R}^n$.

C. Mass-Spring-Damper

The end-effectors grasp the bar on the two sides, as shown in Figure 1. The interaction between each end-effector and the bar is modelled as a mass-spring-damper.

Assuming that at the steady state the end-effector frame $\Sigma_{e,i}$ is coincident with $\Sigma_{b,i}$ the interaction is described by the following equation:

$$\begin{bmatrix} \boldsymbol{f}_{be,i} \\ \boldsymbol{\mu}_{be,i} \end{bmatrix} = \begin{bmatrix} -\boldsymbol{K}_{be,p}(\boldsymbol{p}_{b,i} - \boldsymbol{p}_{e,i}) - \boldsymbol{K}_{be,v}(\boldsymbol{v}_{b,i} - \boldsymbol{v}_{e,i}) \\ -\boldsymbol{K}_{be,o}\theta_{be,i}, \boldsymbol{r}_{be,i} - \boldsymbol{K}_{be,\omega}(\boldsymbol{\omega}_{b,i} - \boldsymbol{\omega}_{e,i}) \end{bmatrix} \tag{3}$$

where $\{\theta_{be,i}, \boldsymbol{r}_{be,i}\}$ are the axis-angle representation of the misalignment between $\Sigma_{e,i}$ and $\Sigma_{b,i}$, $\boldsymbol{K}_{be,p}, \boldsymbol{K}_{be,o} \in \mathbb{R}^{3\times 3}$ are respectively the linear and angular spring coefficient, and $\boldsymbol{K}_{be,v}, \boldsymbol{K}_{be,\omega} \in \mathbb{R}^{3\times 3}$ are respectively the linear and angular damping coefficient.

D. Cooperation

The bar motion is *controlled* by two wrenches applied by the UVMSs end-effectors at the bar ends. The relation between the applied wrenches and the wrench at the bar Center of Mass (CoM) $\boldsymbol{\tau}_b$ is

$$\begin{bmatrix} \boldsymbol{\tau}_{e,1} \\ \boldsymbol{\tau}_{e,2} \end{bmatrix} = \begin{bmatrix} \boldsymbol{W}^{\dagger} & \boldsymbol{V} \end{bmatrix} \begin{bmatrix} \boldsymbol{\tau}_b \\ \boldsymbol{\tau}_{b,int} \end{bmatrix} = \boldsymbol{U} \begin{bmatrix} \boldsymbol{\tau}_b \\ \boldsymbol{\tau}_{b,int} \end{bmatrix} \tag{4}$$

where $\boldsymbol{\tau}_{b,int}$ are the internal forces, i.e., the forces that do not cause movement to the bar.

The pseudo-inverse of the grasping matrix $\boldsymbol{W}$ and a span of its null space $\boldsymbol{V}$ can be defined as,[6]:

$$\boldsymbol{W}^{\dagger} = \frac{1}{2} \begin{bmatrix} \boldsymbol{I}_3 & \boldsymbol{O}_3 \\ \boldsymbol{S}(\boldsymbol{r}_1) & \boldsymbol{I}_3 \\ \boldsymbol{I}_3 & \boldsymbol{O}_3 \\ \boldsymbol{S}(\boldsymbol{r}_2) & \boldsymbol{I}_3 \end{bmatrix}, \boldsymbol{V} = \begin{bmatrix} -\boldsymbol{I}_3 & \boldsymbol{O}_3 \\ -\boldsymbol{S}(\boldsymbol{r}_1) & -\boldsymbol{I}_3 \\ \boldsymbol{I}_3 & \boldsymbol{O}_3 \\ \boldsymbol{S}(\boldsymbol{r}_2) & \boldsymbol{I}_3 \end{bmatrix} \tag{5}$$

where $\boldsymbol{r}_i = \boldsymbol{p}_b - \boldsymbol{p}_{e,i}$ is the vector pointing from the bar CoM to the i-th end-effector frame, and $\boldsymbol{S}(\cdot) \in \mathbb{R}^{3\times 3}$ is the Skew-symmetric matrix.

III. Proposed scheme

In designing a possible control architecture for the cooperative transportation of an object by two UVMSs the specifics characteristics of this environment have been taken into account. Figure 2 shows the overall scheme which is characterized by:

- The object controller which receives in input the object configuration and outputs desired wrenches at the two grasping points. The controller can be designed by resorting to the preferred approach for 6DOF rigid bodies. In this case, to avoid the need to know the object dynamic parameters, a quaternion-based-PID-like action has been implemented;
- The two force controllers which receive in input the desired and measured end-effector wrenches. A simple PI controller is implemented to transform the wrench error in the a desired end-effector trajectory;
- A task-priority inverse kinematics scheme. Any redundancy resolution may be implemented as, e.g., [29], or [19] which, beyond the priority paradigm, also allow to control some variables in a range rather than to a precise value. The output of this block is the reference vehicle and joint positions;
- A low level dynamic controller for the vehicle and the arm. It is worth noticing that coordinate or independent controllers may be implemented since kinematic and dynamic loops are kept separate. In this case, a vehicle controller which adapts with respect to the current, the buoyancy and the sole arm gravity/buoyancy has been implemented [2] while the arm is assumed to be controlled with a PID at joints;

As clear from the description above, the design assumes realistic conditions and, e.g., does not require knowledge of the UVMS dynamic parameters. Also, the choice to implement basic control loops is intentional in order to proof the efficiency of the overall control architecture. Advanced control approaches such as, e.g., model-based coordinated vehicle-arm controllers, may be easily integrated and would allow to achieve superior performances in terms of tracking errors.

The purpose of the paper is develop a cooperative control to transport an object. This operation can also be achieved using a pure positional control, then transpose the desired bar pose on both the end-effectors, eventually an impedance filter to make the operation smoother. In such cases, however, the internal wrench is not controlled, which may result in grasp loss or object breaking.

The idea of the proposed approach come out from a very *simple* approach: a desired bar movement and the internal wrench are converted in desired wrench on the bar ends (detailed in Sect. III-A). In the following the desired wrenches on the end-effectors are converted on a desired end-effector movement (detailed in Sect. III-B) which is controlled with standard control techniques for redundant robotic systems.

Another useful feature coming from the modularity of the design is the possibility to debug separately the various part of the code. Redundancy resolution, for example, can be implemented and tuned by resorting to a *kinematic* model of the problem at hand. Similarly, the low level controller can be debugged separated from any interaction and inverse kinematics issues. The gain tuning is not independent, it is necessary that each loops *sees* as instantaneous the inner one and thus, starting from the inner loop to the outer, it is needed that the bandwidth is decreasing.

A version of this controller for a single UVMS involved in interaction is given in [3].

A. Virtual Bar control

The virtual bar control has the role to generate the desired wrench of both the end-effectors. First of all, we want to generate the desired wrench at the bar CoM, it can be computed by a PID controller:

$$\tau_b^{des} = \boldsymbol{K}_{b,P}\boldsymbol{e}_b + \boldsymbol{K}_{b,D}\dot{\boldsymbol{e}}_b + \boldsymbol{K}_{b,I}\int \boldsymbol{e}_b \tag{6}$$

where the $\boldsymbol{K}_{b,P}, \boldsymbol{K}_{b,D}$ and $\boldsymbol{K}_{b,I}$ are respectively the proportional, derivative and integral gain matrix $\mathbb{R}^{6\times 6}$, and the

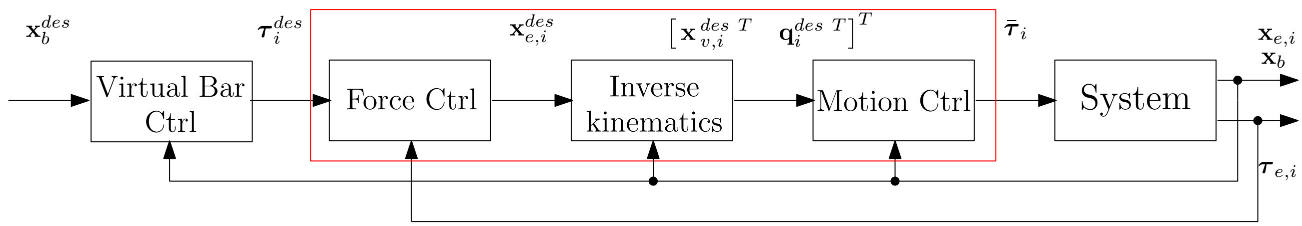

Fig. 2. Block scheme of the overall cooperative transportation controller, where the system is composed by the bar and two UVMS, the red block has been used for each UVMS.

bar error $\boldsymbol{e}_b$:

$$\boldsymbol{e}_b = \begin{bmatrix} \boldsymbol{p}_b^{des} - \boldsymbol{p}_b \\ \eta_b \boldsymbol{\varepsilon}_b^{des} - \eta_b^{des} \boldsymbol{\varepsilon}_b + \boldsymbol{S}(\boldsymbol{\varepsilon}_b^{des}) \boldsymbol{\varepsilon}_b \end{bmatrix} \in \mathbb{R}^6. \tag{7}$$

To control the internal wrench the following equation has been used [6]:

$$\boldsymbol{\tau}_{b,int}^{des} = \boldsymbol{\tau}_{b,int} + \boldsymbol{K}_{int,I} \int (\bar{\boldsymbol{\tau}}_{b,int}^{des} - \boldsymbol{\tau}_{b,int}) \tag{8}$$

where $\bar{\boldsymbol{\tau}}_{b,int}^{des}$ is the constant desired internal wrench, and $\boldsymbol{\tau}_{b,int}$ has been obtained by using the sensed wrenches projected in the null of the grasp matrix inverse. By resorting to eq. (4), the end-effectors wrenches $\boldsymbol{\tau}_{e,i}^{des}$ by using $\tau_b^{des}, \boldsymbol{\tau}_{b,int}^{des}$ can be computed.

B. Force control

A Proportional Integral action is used to stabilize the force error. In fact, being the force signal characterized by a strong noise, its time derivative is usually useless. The force control law is:

$$\boldsymbol{x}_i^{des} = \boldsymbol{K}_{f,P}(\boldsymbol{\tau}_{e,i}^{des} - \boldsymbol{\tau}_{e,i}) + \boldsymbol{K}_{f,I} \int (\boldsymbol{\tau}_{e,i}^{des} - \boldsymbol{\tau}_{e,i}) \tag{9}$$

where $\boldsymbol{K}_{f,P}, \boldsymbol{K}_{f,I} \in \mathbb{R}^{6\times 6}$ are respectively the proportional and integral gains. The idea is to transform the wrench error into an end-effector trajectory.

IV. Numerical simulations

Numerical simulations have been performed to validate the proposed approach. A realistic model has been achieved by resorting to MATLAB and by properly adapting its tool SimMechanics. The system is composed by two UVMSs transporting a bar, as shown in Figure 1. A mass-spring-damper between each end-effector and bar ends has been included as described Section II-C. Both the UVMS have the same structure, they are composed by a fully actuated vehicle, with a 7-DoF manipulator attached. The dynamic parameters of the vehicle have been experimentally identified in [7], while the arm's parameters have been extrapolated by the CAD data. Information about the low level motion control and inverse kinematics approach can be found in [2].

Table II shows the parameters used in simulation, T_c is the sampling time, T_f the simulation duration. The controls gains have been tuned using the following approach. Once measured the inner loop step response time constant. The force control poles have been placed to obtain a time constant one decade of order of magnitude respect the inner loop. The poles of the virtual bar control of another order of magnitude has been increased respect the force control.

The UVMSs are required to transport the bar of :

$$\boldsymbol{p}_b^{des} - \boldsymbol{p}_b = \begin{bmatrix} 0.2 & 0.05 & 0.1 \end{bmatrix}^{\mathrm{T}} [m]. \tag{10}$$

the duration of the trajectory has been of 10 [s], and a trapezoidal velocity profile has been used. The time-line of the bar position/orientation and the corresponding errors are shown in Figure 3.a, where the solid-line are the simulated position and the dotted-line are the desired position. Figure 3.c shows the bar orientation. We can appreciate that the errors in both position and orientation are very low as shown in Figures 3.(b-d).

In all the plots there is an initial error to be recovered due to the intentional mismatching of the controllers parameters.

Figures 4.(a-d) show the wrenches applied on the bar CoM. In detail, the Figure 4.a shows the bar force (solid-lines), the dotted-lines represent the desired force computed on the positional component of the eq. (6). Figure 4.b shows the bar internal force (solid-lines) and the desired internal force $\bar{\boldsymbol{f}}_{b,int}^{des}$. As common, a non-zero value has been imposed. Figure 4.c shows the bar moment (solid-lines), the dotted-lines represent the desired moment computed on the orientation component of the eq. 6. Figure 4.d shows the bar internal moment (solid-lines) and the desired internal moment $\bar{\boldsymbol{\mu}}_{b,int}^{des}$.

Figures 5.(a-b) show the desired and the measured forces $\boldsymbol{f}_{e,i}$ on both the end-effectors.

Parameter	value
T_c	10^{-3} [s]
T_f	30 [s]
UVMS mass	479.2 [kg]
Bar mass	1.5 [kg]
$\boldsymbol{K}_{be,p}$	500
$\boldsymbol{K}_{be,v}$	10
$\boldsymbol{K}_{be,o}$	500
$\boldsymbol{K}_{be,\omega}$	10
$\boldsymbol{K}_{int,I}$	$0.1\boldsymbol{I}_6$
$\boldsymbol{K}_{b,P}$	$\begin{bmatrix}100\boldsymbol{I}_3 & 700\boldsymbol{I}_3\end{bmatrix}^{\mathrm{T}}$
$\boldsymbol{K}_{b,I}$	$\begin{bmatrix}200\boldsymbol{I}_3 & 500\boldsymbol{I}_3\end{bmatrix}^{\mathrm{T}}$
$\boldsymbol{K}_{b,D}$	$\begin{bmatrix}10\boldsymbol{I}_3 & 5\boldsymbol{I}_3\end{bmatrix}^{\mathrm{T}}$
$\boldsymbol{K}_{f,P}$	$10^{-3}\boldsymbol{I}_6$
$\boldsymbol{K}_{f,I}$	$20 \cdot 10^{-3}\boldsymbol{I}_6$

TABLE II

SIMULATION PARAMETERS AND CONTROL GAINS.

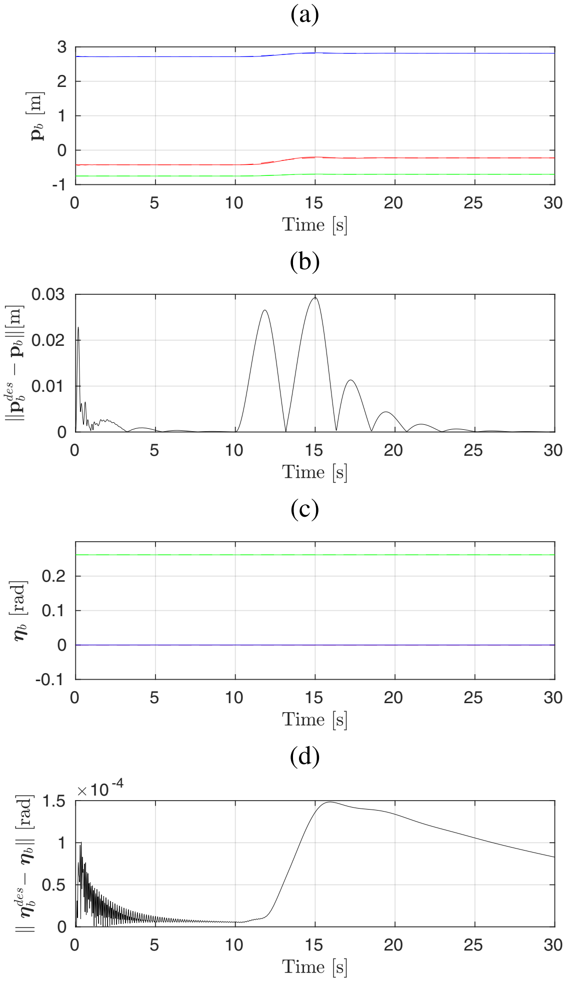

Fig. 3. Time-line of the bar position (a) and orientation (c) and corresponding norms error (b-d). The desired variables are denoted with dotted-lines, the simulated with the solid-lines. The x, y, z-axis are reported (red-green-blue).

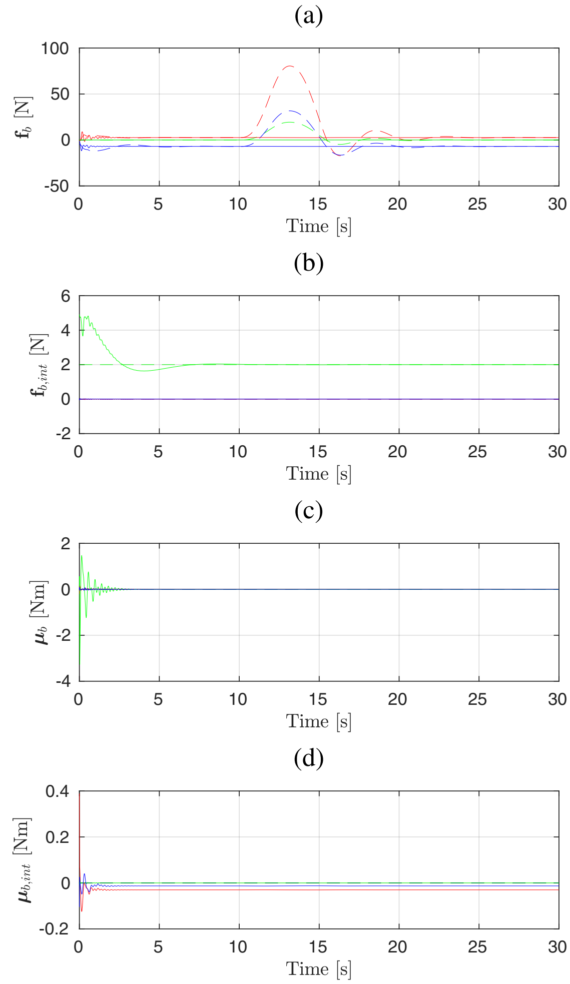

Fig. 4. Time-line of the force and moment on the bar CoM (a-c) and the internal force and moment on the bar CoM are reported in (b-d). The desired variables are denoted with dotted-lines, the simulated with the solid-lines. The x, y, z-axis are reported (red-green-blue).

Figures 6 show the end-effecor 1 position (a) and orientation (b).

V. Conclusions

In this paper we presented a cooperation control approach to transport an object to be performed by two underwater vehicle-manipulator systems. The proposed control is composed by several control loops: the virtual bar control, the control force, the inverse kinematics, and a motion control. The first two blocks are aimed at implementing the interaction control part, while the last two are kinematic and dynamic control. To validate the proposed approach a numerical simulations on a realistic dynamic model has been presented.

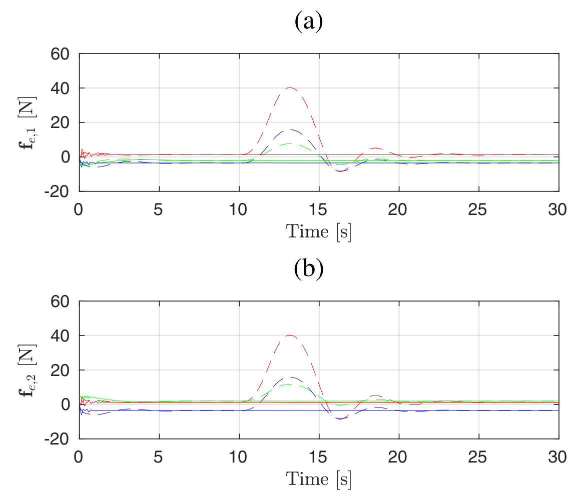

Fig. 5. Time-line of the force on both the end-effectors. The desired variables are denoted with dotted-lines, the simulated with the solid-lines. The x, y, z-axis are reported (red-green-blue).

Acknowledge

This work was supported by the European Community through the projects EUMR (731103-2), ROBUST (H2020-690416) and DexROV (H2020-635491).

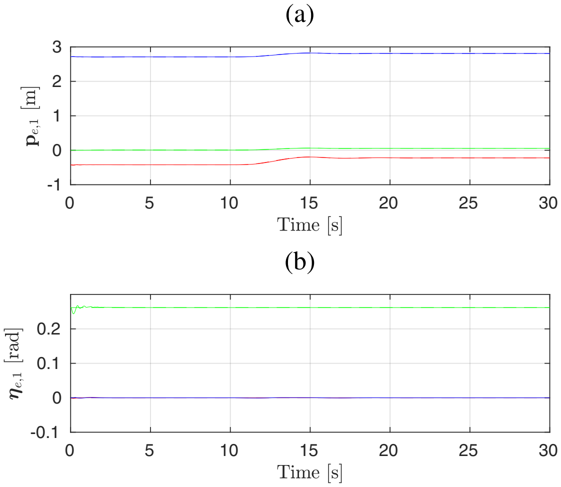

Fig. 6. Time-line of the end-effector position (a) and orientation (b) of the end-effector 1. The desired variables are denoted with dotted-lines, the simulated with the solid-lines. The x, y, z-axis are reported (red-green-blue).

References

[1] G. Antonelli. *Underwater robots*. Springer Tracts in Advanced Robotics, Springer-Verlag, Heidelberg, D, 4th edition, 2018.

[2] G. Antonelli and E. Cataldi. Recursive adaptive control for an underwater vehicle carrying a manipulator. In *Control and Automation (MED), 2014 22nd Mediterranean Conference of*, pages 847–852, June 2014.

[3] G. Antonelli and E. Cataldi. Basic interaction operations for an underwater vehicle-manipulator system. In *ICAR 2015 - 17th International Conference on Advanced Robotics*, Istanbul, T, July 2015.

[4] G. Antonelli, S. Chiaverini, and N. Sarkar. External force control for underwater vehicle-manipulator systems. *IEEE Transactions on Robotics and Automation*, 17(6):931–938, December 2001.

[5] G. Antonelli, N. Sarkar, and S. Chiaverini. Explicit force control for underwater vehicle-manipulator systems. *Robotica*, 20(3):251–260, 2002.

[6] F. Caccavale and M. Uchiyama. Cooperative manipulators. In *Springer handbook of robotics*, pages 701–718. Springer, 2008.

[7] M. Caccia, G. Indiveri, and G. Veruggio. Modeling and identification of open-frame variable configuration unmanned underwater vehicles. *Oceanic Engineering, IEEE Journal of*, 25(2):227–240, 2000.

[8] G. Casalino, D. Angeletti, T. Bozzo, and G. Marani. Dexterous underwater object manipulation via multi-robot cooperating systems. In *Robotics and Automation, 2001. Proceedings 2001 ICRA. IEEE International Conference on*, volume 4, pages 3220–3225, Seoul, Korea, 2001. IEEE.

[9] G. Casalino, M. Caccia, S. Caselli, C. Melchiorri, G. Antonelli, A. Caiti, G. Indiveri, G. Cannata, E. Simetti, S. Torelli, A. Sperindé, F. Wanderlingh, G. Muscolo, M. Bibuli, G. Bruzzone, E. Zereik, A. Odetti, E. Spirandelli, A. Ranieri, J. Aleotti, D.L. Rizzini, F. Oleari, F. Kallasi, G. Palli, U. Scarcia, L. Moriello, and E. Cataldi. Underwater intervention robotics: An outline of the Italian national project MARIS. *Marine Technology Society Journal*, 50(4):98–107, 2016.

[10] P. Di Lillo, E. Simetti, D. De Palma, E. Cataldi, G. Indiveri, G. Antonelli, and G. Casalino. Advanced ROV autonomy for efficient remote control in the DexROV project. *Marine Technology Society Journal*, 50(4):67–80, 2016.

[11] J.J. Fernández, M. Prats, P.J. Sanz, J.C. García, R. Marin, M. Robinson, D. Ribas, and P. Ridao. Grasping for the seabed: Developing a new underwater robot arm for shallow-water intervention. *IEEE Robotics & Automation Magazine*, 20(4):121–130, 2013.

[12] Shahab Heshmati-alamdari, Alexandros Nikou, Kostas J Kyriakopoulos, and Dimos V Dimarogonas. A robust force control approach for underwater vehicle manipulator systems. *IFAC-PapersOnLine*, 50(1):11197–11202, 2017.

[13] H. Kajita and K. Kosuge. Force control of robot floating on the water utilizing vehicle restoring force. In *Intelligent Robots and Systems, 1997. IROS'97., Proceedings of the 1997 IEEE/RSJ International Conference on*, volume 1, pages 162–167, Grenoble, France, 1997. IEEE.

[14] O. Khatib. A unified approach for motion and force control of robot manipulators: The operational space formulation. *IEEE Journal of Robotics and Automation*, 3(1):43–53, 1987.

[15] O. Khatib, X. Yeh, G. Brantner, B. Soe, B. Kim, S. Ganguly, H. Stuart, S. Wang, M. Cutkosky, A. Edsinger, et al. Ocean One. *IEEE Robotics & Automation Magazine*, 2016.

[16] O. Khatib, K. Yokoi, K. Chang, D. Ruspini, R. Holmberg, and A. Casal. Vehicle/arm coordination and multiple mobile manipulator decentralized cooperation. In *Intelligent Robots and Systems' 96, IROS 96, Proceedings of the 1996 IEEE/RSJ International Conference on*, volume 2, pages 546–553, Osaka, Japon, 1996. IEEE.

[17] S. Lemieux, J. Beaudry, and M. Blain. Force control test bench for underwater vehicle-manipulator system applications. In *IEEE Industrial Electronics, IECON 2006 - 32nd Annual Conference on*, pages 4036–4042, 2006.

[18] N. Manerikar, G. Casalino, E. Simetti, S. Torelli, and A. Sperindé. On autonomous cooperative underwater floating manipulation systems. In *Robotics and Automation (ICRA), 2015 IEEE International Conference on*, pages 523–528. IEEE, 2015.

[19] S. Moe, G. Antonelli, A. Teel, K. Pettersen, and J. Schrimpf. Set-based tasks within the singularity-robust multiple task-priority inverse kinematics framework: General formulation, stability analysis and experimental results. *Frontiers in Robotics and AI*, 3:16, 2016.

[20] J. Nakanishi, R. Cory, M. Mistry, J. Peters, and S. Schaal. Operational space control: A theoretical and empirical comparison. *The International Journal of Robotics Research*, 27(6):737–757, 2008.

[21] E. Olguin-Diaz, G. Arechavaleta, G. Jarquin, and V. Parra-Vega. A passivity-based model-free force–motion control of underwater vehicle-manipulator systems. *IEEE Transactions on Robotics*, 2013.

[22] N. Palomeras, A. Carrera, N. Hurtós, G.C. Karras, C.P. Bechlioulis, M. Cashmore, D. Magazzeni, D. Long, M. Fox, K. Kyriakopoulos, et al. Toward persistent autonomous intervention in a subsea panel. *Autonomous Robots*, 40(7):1279–1306, 2016.

[23] N. Palomeras, A. Penalver, M. Massot-Campos, G. Vallicrosa, P. Negre, J.J. Fernández, P. Ridao, P.J. Sanz, G. Oliver-Codina, and A. Palomer. I-AUV docking and intervention in a subsea panel. In *Intelligent Robots and Systems (IROS 2014), 2014 IEEE/RSJ International Conference on*, pages 2279–2285. IEEE, 2014.

[24] M. Prats, D. Ribas, N. Palomeras, J.C. García, V. Nannen, S. Wirth, J.J. Fernández, J.P. Beltrán, R. Campos, P. Ridao, et al. Reconfigurable AUV for intervention missions: a case study on underwater object recovery. *Intelligent Service Robotics*, 5(1):19–31, 2012.

[25] J. Shao, L. Wang, and J. Yu. Development of an artificial fish-like robot and its application in cooperative transportation. *Control Engineering Practice*, 16(5):569–584, 2008.

[26] B. Siciliano, L. Sciavicco, L. Villani, and G. Oriolo. *Robotics: modelling, planning and control*. Springer Verlag, 2009.

[27] E. Simetti and G. Casalino. Manipulation and transportation with cooperative underwater vehicle manipulator systems. *IEEE Journal of Oceanic Engineering*, 2016.

[28] E. Simetti, G. Casalino, N. Manerikar, A. Sperindé, S. Torelli, and F. Wanderlingh. Cooperation between autonomous underwater vehicle manipulations systems with minimal information exchange. In *OCEANS 2015-Genova*, pages 1–6. IEEE, 2015.

[29] E. Simetti, G. Casalino, S. Torelli, A. Sperindé, and A. Turetta. Floating underwater manipulation: Developed control methodology and experimental validation within the TRIDENT project. *Journal of Field Robotics*, 31(3):364–385, 2013.

[30] Y.C. Sun and C.C. Cheah. Coordinated control of multiple cooperative underwater vehicle-manipulator systems holding a common load. In *OCEANS'04. MTTS/IEEE TECHNO-OCEAN'04*, volume 3, pages 1542–1547, Kobe, Japan, 2004. IEEE.

[31] D. Youakim, P. Ridao, N. Palomeras, F. Spadafora, D. Ribas, and M. Muzzupappa. Autonomous underwater free-floating manipulation using MoveIt! *IEEE Robotics & Automation Magazine*, 2017.